Electronic Supplementary Material (ESI) for ChemComm.

Supporting Information

2D Hybrid Perovskite Incorporating Cage-Confined Secondary Ammonium Cation toward Effective Photodetection

Lina Hua, Huaixi Chen, Shiguo Han, Haojie Xu, Lei Lu, Liwei Tang, Beibei Wang, Junhua Luo and Zhihua Sun*

1. Experimental section

Synthesis and Characterization of (*i*-BA)$_2$(DMA)Pb$_2$Br$_7$: All the chemical reagents were purchased from commercial suppliers and used without further purification. A mixture of *n*-isobutylamine (98% *wt*), dimethylamine (98% *wt*) and lead acetate trihydrate (the molar ratio: 2:1:2) dissolved in concentrated HBr (48 % *wt*) were placed in a glass vial by heating, forming a bright yellow solution. The temperature-cooling technique was utilized to control the crystal growth. Large yellow bulk crystals grew in an oven, of which the initial temperature was set at 80℃ and the cooling rate was 0.5°C per day. Powder X-ray diffractometry (PXRD) data were measured at room temperature, using a Mini Flex II Powder X-ray diffractometer. The UV−vis absorption spectra were recorded with a PerkinElmer Lambda 950 UV-vis-IR Spectrophotometer. Thermogravimetric analyses (TGA) were performed in the range of 300-1200 K using the STA449C Thermal Analyser. Calculations on the band structures and partial density of states were performed with the single-crystal structure data by the total energy code CASTEP in the framework of DFT. The general gradient approximation functional of Perdew–Burke–Ernzerhof was employed. The core–electrons interactions were described by the norm-conserving pseudopotentials. The other parameters and convergent criteria were the default values of CASTEP code.

Crystal Structure Determination: The single crystal X-ray diffractions were measured on a Bruker D8 diffractometer with Mo Kα radiation (λ = 0.77 Å) at 330 K. The crystal

structure of $IA)_2(DMA)Pb_2Br_7$ was solved by using the direct methods and refined by the full-matrix method based on F^2 using the SHELXS-97 software package. As for the non-hydrogen atoms, the different Fourier maps and anisotropical refinement were performaned by using SHELXL- 97. Crystal data, structure refinements, and selected parameters are listed in Tables S1–S4 (Supporting Information).

Fabrication and Measurements of Photodetectors: The planar array photodetectors were fabricated on the high-quality crystal wafers. A square copper mesh was used as a mask to get the patterned Au electrode. The channel length (L) and width (W) of the device were 230 and 30 μm, respectively. The *I-V* measurements were performed using a Keithley 6517B source meter on a probe station (EverBeing, PE4). Laser diodes with 405 nm (LP405-SF10) were used as light source by applying a voltage of 10 V. The power intensity of light sources was carefully measured using a power meter (Thorlabs GmbH., PM 100D). The steady state response time was carried by illuminating the sample with a 405 nm laser, the high-speed Tektronix MDO3014 Oscilloscope was used to record the output. For polarization-sensitive photodetection, the linearly polarized light was obtained through a half-wave plate, and then rotate the half-wave plate during the measurement. All measurements were performed in ambient conditions at room temperature.

Figures

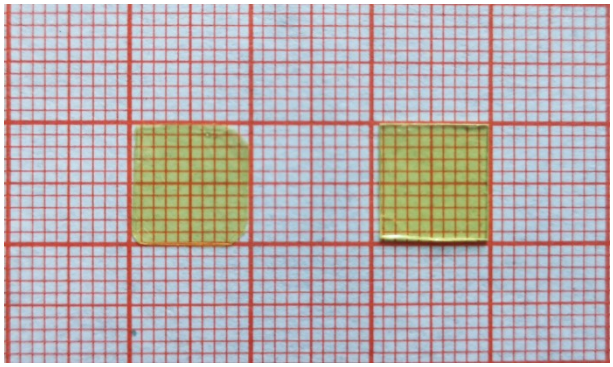

Figure S1. Bulk crystal of **1** with the dimension of 10 × 9 × 2 mm^3.

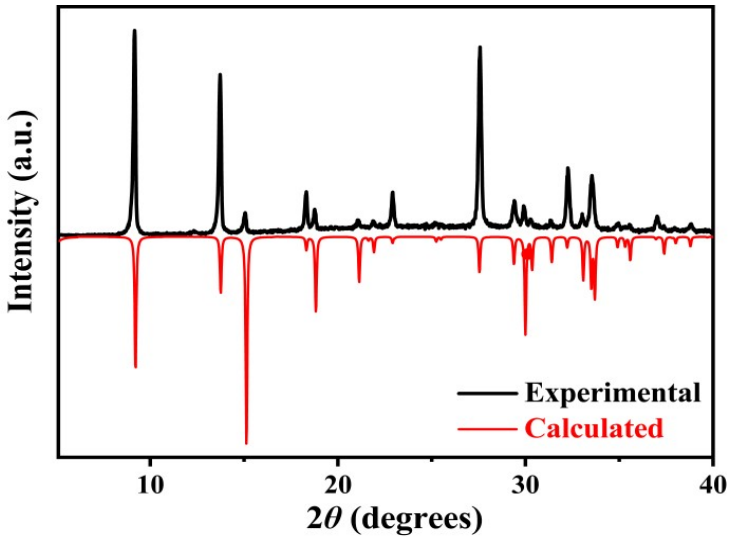

Figure S2. Experimental and calculated powder X-ray diffraction patterns of **1** at room temperature.

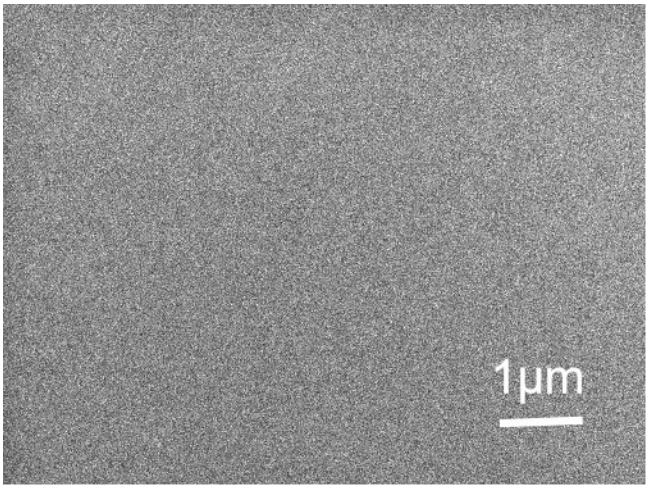

Figure S3. SEM image of crystal surface for **1**.

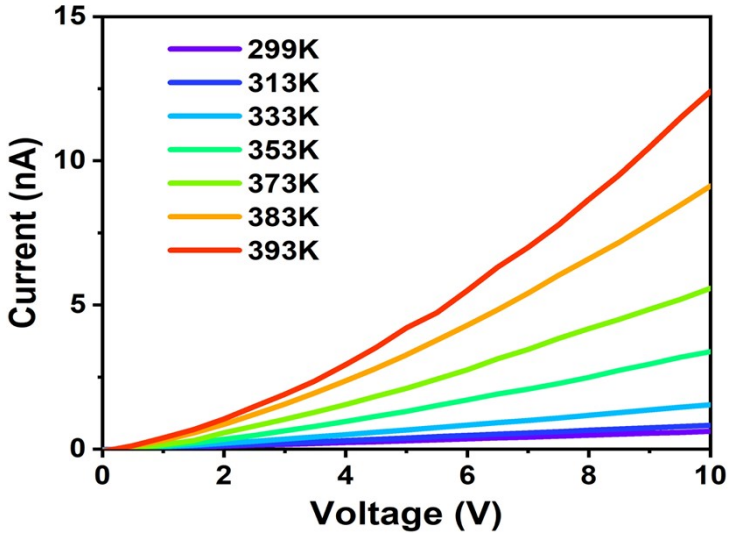

Figure S4. The current–voltage graphs measured at different temperatures.

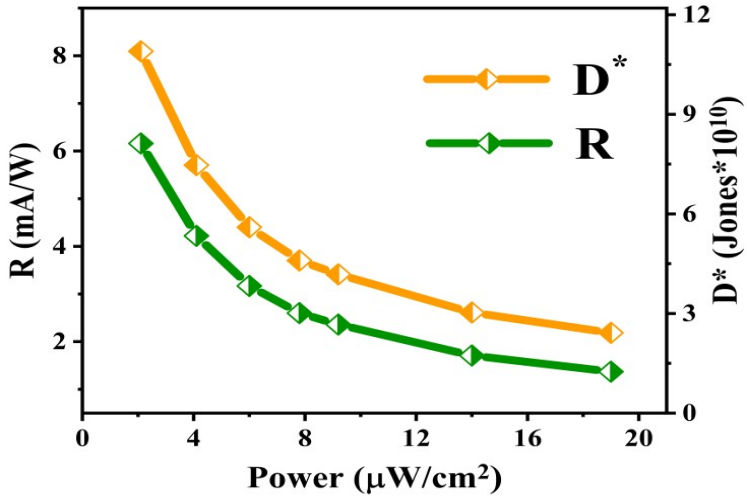

Figure S5. Responsivity and detectivity as a function of the incident light intensity based on the single-crystal photodetector.

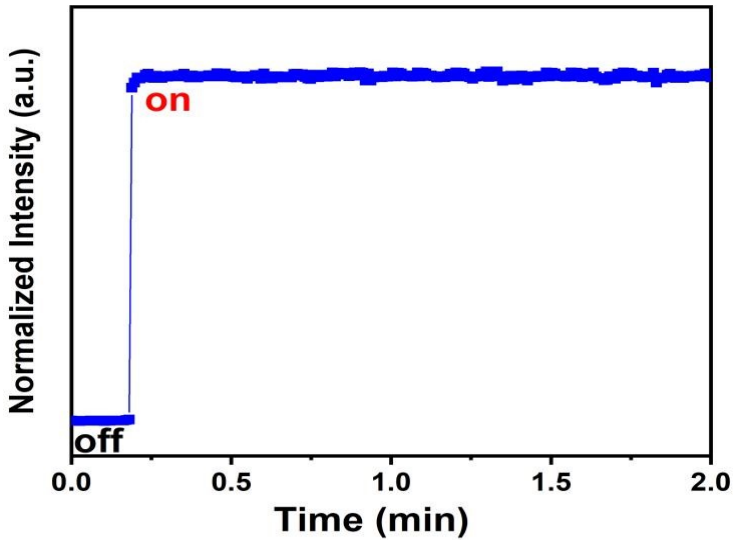

Figure S6. The stability test of the device under constant illumination.

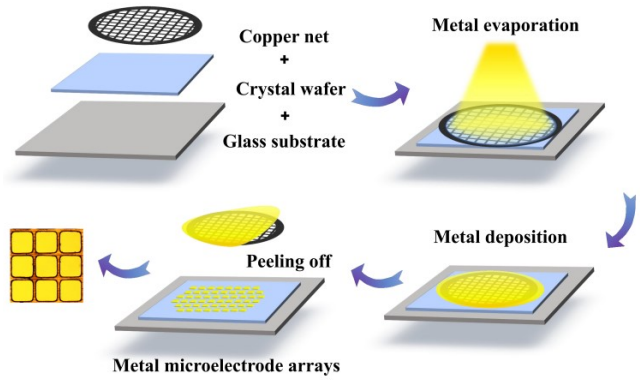

Figure S7. Schematic illustration of the photodetector based on the high-quality bulk crystal of **1**.

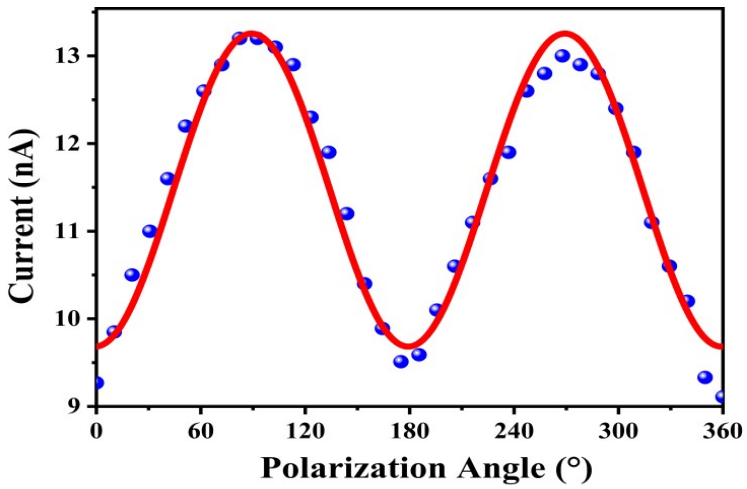

Figure S8. Polarization-dependence of photocurrents for **1**.

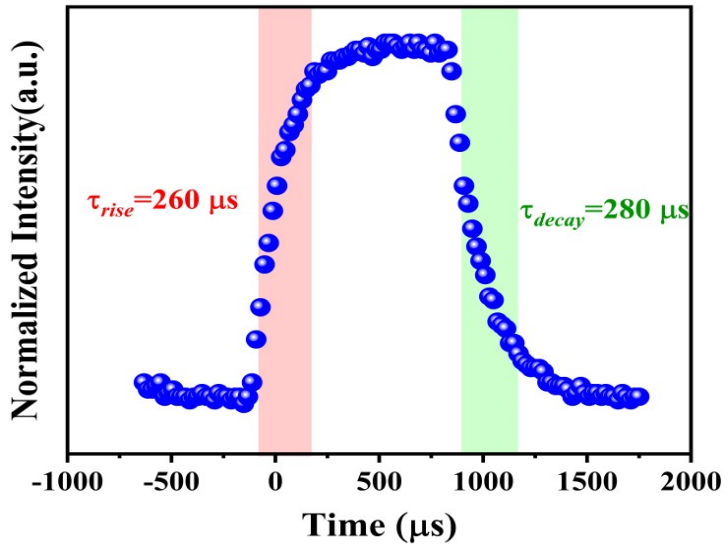

Figure S9. Rise and fall process of photocurrent responses during on/off illumination switching.

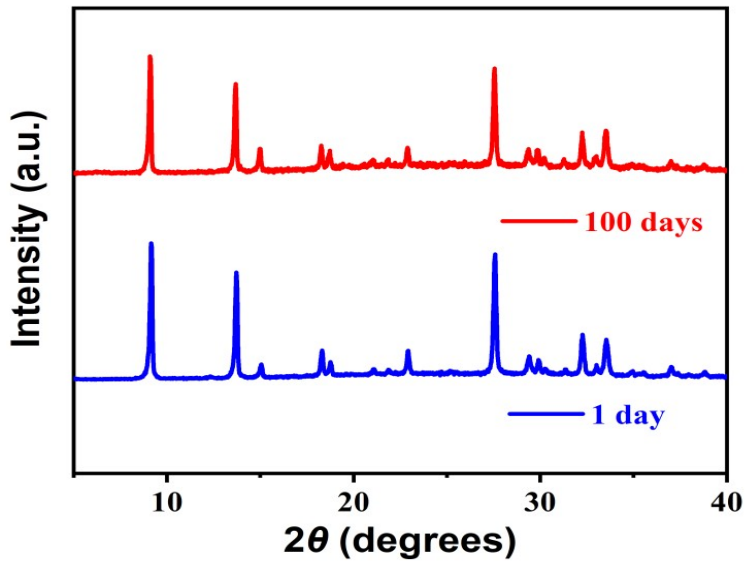

Figure S10. Powder X-ray diffraction patterns of **1** recorded on the sample after one day and 100 days.

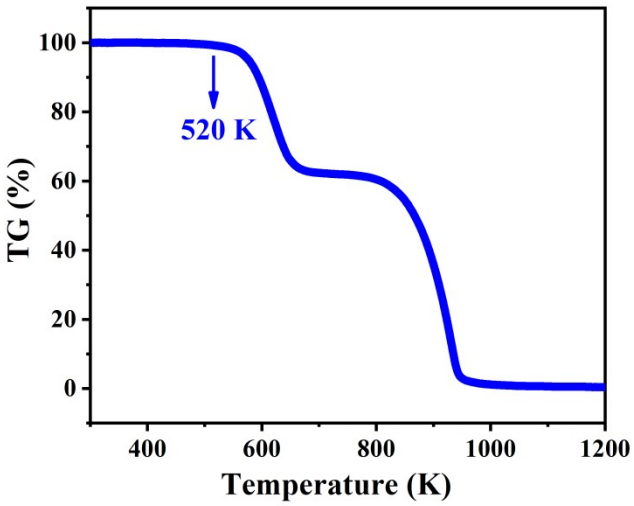

Figure S11. TG curve shows the thermal stability of **1** up to 520 K.

Table S1. Crystal data and structure refinement for **1**.

	Room Temperature Date	**High Temperature Date**
Empirical formula	$C_{10}H_{32}Br_7N_3Pb_2$	$C_{10}H_{32}Br_7N_3Pb_2$
Formula weight	1168.13	1168.13
Temperature/K	299 K	330 K
Crystal system	tetragonal	tetragonal
Space group	*I*4/*mmm*	*I*4/*mmm*
a/Å	6.0037(11)	5.9841(2)
b/Å	6.0037(11)	5.9841(2)
c/Å	39.308(13)	39.049(3)
α/°	90	90
β/°	90	90
γ/°	90	90
Volume/ Å^3	1416.8(7)	1398.33(14)
Z	2	2
ρ_{calcg} / cm^3	2.738	2.774
μ / mm^{-1}	21.738	22.025
F(000)	1044.0	1044.0
Radiation	MoKα (λ = 0.71073)	MoKα (λ = 0.71073)
2θ range for data collection/°	6.866 to 54.524	6.26 to 55.144
Index ranges	-7 ≤ *h* ≤ 7, -7 ≤ *k* ≤ 7, -50 ≤ *l* ≤ 49	-6 ≤ *h* ≤ 7, -7 ≤ *k* ≤ 7, -50 ≤ *l* ≤ 46
Independent reflections	541 [R_{int} = 0.0453, R_{sigma} = 0.0311]	545 [R_{int} = 0.0490, R_{sigma} = 0.0328]
Goodness-of-fit on F^2	1.409	1.194
Data/restraints/parameters	541/97/91	545/18/50
Final R indexes [I> = 2σ	R_1 = 0.0913,	R_1 = 0.0741,

(I)]	wR_2 = 0.2812	wR_2 = 0.2190
Final R indexes [all data]	R_1 = 0.0962, wR_2 = 0.2910	R_1 = 0.0791, wR_2 = 0.2262
Largest diff. peak/hole/eÅ^{-3}	1.79/-3.35	1.81/-2.12

Table S2. Bond lengths for **1**

Atom	Atom	Length/Å	Atom	Atom	Length/Å
Pb1	Br3	3.0051(6)	C1	C2	1.502(12)
Pb1	Br2	2.835(3)	C1	N1	1.513(14)
Pb1	Br1	3.2063(12)	C4	C2	1.497(12)
C5	N2	1.501(13)	C2	C3	1.500(11)
N2	C6	1.501(13)			

[1]1-Y,+X,+Z; [2]1-Y,1+X,+Z; [3]1+X,+Y,+Z

Table S3. Bond Angles for **1**.

Atom	Angle/	Atom	Angle/
Br3-Pb1-Br3[1]	89.875(5)	Pb1-Br1-Pb1[5]	180.0
Br3-Pb1-Br3[2]	174.64(10)	C6-N2-C5	112.6(10)
Br3-Pb1-Br1	92.68(5)	C2-C1-N1	112.1(11)
Br2-Pb1-Br3[1]	87.32(5)	C4-C2-C1	97.7(8)
Br2-Pb1-Br1	180.0	C4-C2-C3	113.2(10)
Pb1[4]-Br3-Pb1	174.65(10)	C3-C2-C1	129.9(13)

[1]-Y,+X,+Z; [2]1-Y,+X,+Z; [3]+X,1+Y,+Z; [4]+X,-1+Y,+Z; [5]1-X,1-Y,1-Z

Table S4. N-H···I hydrogen bonds of **1**.

D-H	d(D-H)	d(H..A)	<DHA	d(D..A)	A
N2[a]-H2B[a]	0.910	2.964	138.41	3.694	Br3[-y+1, x, z]
N1[a]-H1D[a]	0.910	2.585	151.56	3.413	Br3 [-y+1, x, z]
N1[a]-H1E[a]	0.910	2.731	151.39	3.556	Br3[x, y-1, z]